Results in Surfaces and Interfaces 14 (2024) 100191

Contents lists available at ScienceDirect

Results in Surfaces and Interfaces

journal homepage: www.elsevier.com/locate/rsurfi

The effects of NaCl addition on the particle-bubble interactions of galena in the presence of xanthate

Anna M. Nowosielska [a], Aleksandar N. Nikoloski [a], Drew F. Parsons [a,b,*]

[a] Harry Butler Institute (Centre for Water, Energy and Waste), College of Science, Health, Engineering and Education (Engineering and Energy), Murdoch University, 90 South St, Murdoch, WA 6150, **Australia**

[b] Department of Chemical and Geological Sciences, University of Cagliari, Cittadella Universitaria, 09042 Monserrato, CA, **Italy**

ARTICLE INFO

Keywords:
Flotation
Galena
Xanthate
Chemisorption
Total interaction energy

ABSTRACT

This work investigated the effects of NaCl addition on galena flotation in the presence of xanthate. The micro-flotation experiments were performed using NaCl solutions which also included xanthate, at pH 9 (±0.1). Our results indicated that galena recovery improved for higher NaCl as well as higher xanthate concentrations.

A pH-dependent chemisorption model for the galena surface, with the addition of xanthate adsorption was calibrated using measured zeta potential values. We propose that xanthate adsorption on galena can take place via two separate mechanisms. The first mechanism involves direct xanthate chemisorption to specific surface sites. The second mechanism involves lead/xanthate complexes formed in the bulk solution. These lead/xanthate complexes attach on the galena surface as hydrophobic lead xanthate salts.

The galena-air bubble interactions are repulsive in 1 mM NaCl, with or without xanthate, consistent with the lower galena recovery measured experimentally. An increase to 100 mM NaCl, irrespective of the xanthate addition, resulted in attractive galena-air bubble total interaction energies. The agreement with the experimental results shows the effectiveness of the charge regulated model for estimating the galena and air bubble behaviours during flotation in NaCl solutions.

1. Introduction

Due to a limited supply of fresh water, the ability to utilise seawater or recycled water containing additional ions is of major importance in the mineral industry. Previous investigations documented that these increasing concentrations of dissolved ionic species in solution can have a positive impact on the solid-gas and the liquid-gas interfaces in flotation (Castro et al., 2013; Hancer et al., 2001; Lucay et al., 2015; Ramos et al., 2013; Smith and Heyes, 2012). This has mainly been attributed to the changes in the hydrogen bonding networks (Wu et al., 2016), or in other words, the changes in ways ionic species interact with the water structures. The increased electrolyte concentration in solution helps to facilitate particle-bubble attachment by reducing the energy barrier via a compression of the ionic diffuse layers between a particle and bubble (Harvey et al., 2002; Laskowski and Castro, 2015). It is speculated that the efficiency of the mineral recovery depends on the nature of the ionic species present in solution as well as their absolute concentrations (Wu et al., 2016). However, the process mechanisms are still not clear, therefore, further research of the combined effects of ionic species on mineral flotation, especially from a theoretical angle is needed.

The effectiveness of mineral flotation depends on the number of successful particle-bubble attachments. When particles have hydrophilic (water-attracting) rather than hydrophobic (water-repellent) surface characteristics, it may be necessary to use reagents such as collectors to control and maintain the selectivity of the flotation process. Xanthates are the commonly used collectors for sulfide minerals due to their low affinity for most non-sulfide gangue minerals. The chemical structure of a xanthate collector consists of a polar group, which can attach to the surface of a mineral particle, and a nonpolar hydrophobic hydrocarbon chain. Collector adsorption may take place by physical forces (physisorption) via an ion exchange at the mineral particle-collector interface within the electric double layer (Abaka-Wood et al., 2017) or by chemical bonding (chemisorption). Buckley and Woods (1994) proposed that chemisorption will be the initial reaction between galena and xanthate which will result in xanthate attaching to the positively charged lead atoms in the galena matrix. Lead dixanthate will be the hydrophobic product formed on the surface of galena following xanthate

* Corresponding author. Department of Chemical and Geological Sciences, University of Cagliari, Cittadella Universitaria, 09042 Monserrato, CA, **Italy**.
E-mail address: drew.parsons@unica.it (D.F. Parsons).

https://doi.org/10.1016/j.rsurfi.2024.100191
Received 2 October 2023; Received in revised form 23 January 2024; Accepted 29 January 2024
Available online 12 February 2024

chemisorption (Hu et al., 2020). According to Woods (2003), collectors are most efficient when they bond via chemisorption because it allows for a monolayer of xanthate to be formed on the mineral surface before multilayers of lead dixanthate form in the bulk. It has also been noted that chemisorbed xanthate is less soluble than the bulk lead dixanthate (Buckley and Woods, 1994). Zeta potential measurements are often employed to study the extent of the collector adsorption on the mineral surface (Abaka-Wood et al., 2017; Jordens et al., 2013). Collector adsorption is described as chemisorption if the value of the isoelectric point (IEP) changes because of collector addition (Han et al., 1973) and is indicated by a shift in the measured zeta potential values.

Majority of studies found in the literature focus on investigating the collector adsorption on a mineral surface in freshwater flotation (Grano et al., 1997; Xing et al., 2017; Han et al., 2019; Hu et al., 2020). However, with more flotation plants making use of process waters containing additional ions, there is a need for further research into the effects of water quality on the collector adsorption and mineral recovery.

Several studies reported on the effects of saline water/seawater on the mineral recovery and the size of the bubbles during flotation. Table 1 presents a summary of some of these studies.

The main objective of this study was to evaluate the effects of NaCl on galena flotation in the presence of xanthate. This work builds upon our recently published study on the effects of NaCl on the flotation of galena (Nowosielska et al., 2022a), while focusing on the combining effects of salts (NaCl and xanthate) during galena flotation. The recovery of unoxidized fresh galena was investigated using micro-flotation experiments, zeta potential measurements as well as contact angle measurements. These were compared with predictions from theoretical models for galena-bubble interactions. The results presented in this work not only contribute to the greater understanding of the mechanisms involved in xanthate adsorption on galena in NaCl solutions, but also provide more insight into galena-air bubble interactions during flotation in NaCl solutions.

Table 1
A summary of the literature review on the effects of saline water/seawater on the sulfide mineral flotation and bubble size.

YEAR	STUDY	FINDINGS
1967	Marrucci and Nicodemo (Marrucci and Nicodemo, 1967)	Increased repulsions at the bubbles surface sites due to the presence of salt ions in solution
1970	Laskowski and Iskra (Laskowski and Iskra, 1970)	Higher mineral recoveries at higher salt concentrations linked to the faster rupturing of the water film between particles and bubbles
2015	Laskowski and Castro (Laskowski and Castro, 2015)	
2016	Jaldres et al. (Jeldres et al., 2016)	
1983	Furstenau et al. (Fuerstenau et al., 1983)	Faster flotation rate due to higher salt concentration in solution
1986	Dobby and Finch (Dobby and Finch, 1986)	Smaller bubble size in higher ionic concentrations leads to higher collision and attachment efficiency and higher mineral recoveries
1989	Yoon and Sabey (Yoon et al., 1989)	Flotation in highly concentrated electrolyte solutions introduced faster flotation kinetics
1993	Craig et al. (Craig et al., 1993a)	Smaller bubble size in salt solutions shown to promote the stability of the froth phase
2004	Nguyen and Schulze (Nguyen and Schulze, 2004)	Higher mineral recoveries attributed to a shorter induction time as the solution ionic strength increases
2008	Zhang et al. (Zhang et al., 2008)	Increased solution salinity caused air precipitation on the mineral surface and resulted in the formation of nano-bubbles. These non-bubbles have been shown to improve particle-bubble attachment efficiency.
1980	Peakock and Matijević (Peacock and Matijević, 1980)	Seawater reduced the solubility of ionic surfactants during mineral flotation and resulted in lower mineral recoveries
2012	Yu et al. (Yu et al., 2012)	
2018	Chang et al. (Chang et al., 2018)	
2013	Liu et al. (Liu et al., 2013)	Higher salt concentration in solution leads to higher bubble surface area flux, which helps to increase the possibility of particle-bubble attachments
1995	Grano et al. (Grano et al., 1995)	Flotation using seawater resulted in lower mineral recoveries due to particles becoming more hydrophilic
2012	Ikumapayi et al. (Ikumapayi et al., 2012)	
2013	Ramos et al. (Ramos et al., 2013)	
2013	Castro et al. (Castro et al., 2013)	The addition of NaCl helped with froth stabilization and bubble size reduction
2014	Quinn et al. (Quinn et al., 2014)	
2014	Wang and Peng (Wang and Peng, 2014)	Compression of the ionic diffuse layers due to an increase in NaCl concentration in solution has a positive effect on the particle-bubble interactions during flotation
2015	Boujounoui et al. (Boujounoui et al., 2015)	In seawater flotation, the competitive adsorption between xanthate and SO_4^{2-} produced lower mineral recoveries
2017	Elizondo-Alvarez et al. (Elizondo-Alvarez et al., 2017)	Evidence of surface passivation by SO_4^{2-} ions during seawater flotation

2. Materials and methods

2.1. Materials

The galena mineral sample came from Broken Hill South Mine (Broken Hill, NSW). A multi-elemental analysis, determined by Inductively Coupled Plasma – Mass Spectrometry (ICP-MS) indicated a high purity galena sample of ~99.03% (~85.61% Pb and ~13.52% S). All experiments were performed using deionised (DI) water at room temperature. Analytical grade (≥99%) sodium chloride (NaCl) (Sigma-Aldrich) was used to adjust the ionic strength of each test solution to 1, 10 or 100 mM NaCl. Analytical grade (≥98%) sodium hydroxide (NaOH) (Sigma-Aldrich) and 32 % hydrochloric acid (HCl) (Sigma-Aldrich) were used to regulate the pH. The collector solutions were made using sodium ethyl xanthate ($C_3H_5NaOS_2$) (≥97%, Fisher Scientific) at 1 or 10 mM.

The galena feed size distribution was determined by a laser diffraction particle size analyser (Microtrac S3500). The P_{50}, representing the "median galena particle diameter" for the distribution was calculated to be around 53 μm, with a P_{80} of ~85 μm.

2.2. Methods

2.2.1. 2.2.1 Contact angle measurements

The surface of a hand-picked sample of galena was polished using 800 and 1200 grit silicon carbide papers, with the surface rinsed with deionised (DI) water between polishes. We kept the time between galena surface preparation and contact angle measurements to a minimum (within minutes) to minimise any impact of galena surface oxidation, which is rapid within the first 120 min of exposure to air (Fornasiero et al., 1994; Ralston, 1994). By using a micro-pipette, a stable liquid drop was deposited on the sample surface. The image of the angle the liquid drop makes with the surface of galena was captured and analysed using the OpenDrop software (Berry et al., 2015). We measured the contact angles on freshly polished galena surfaces for solutions which contained NaCl salt (1, 10 or 100 mM) only, or NaCl salt and sodium ethyl xanthate (1 or 10 mM), at pH 9 (±0.1). Here, the contact angles were measured using solutions at pH 9 (±0.1), the same as that used in the micro-flotation experiments. The results from these measurements assisted in examining the surface wettability properties of a freshly prepared galena sample. For each test condition, at least three measurements were performed to minimise the error. All contact angles were measured at room temperature (25 ± 2 °C).

2.2.2. Zeta potential measurements

Prior to performing the measurements, dilute mixtures (~0.5–1 % solids) of 1 mM or 10 mM NaCl (with the addition of 1 mM sodium ethyl xanthate) and fine galena particles (~5 μm) were prepared. Using HCl or NaOH, the pH of each test solution was adjusted from pH 2 to pH 10. Around 1 mL of each solution sample was transferred to a Malvern Dip Cell which was then placed in a Malvern Nano-ZS90 zeta potential analyser (Malvern Instruments Ltd., Malvern, UK). At least three measurements were taken for each test solution. All zeta potential measurements were carried out at room temperature.

2.2.3. Micro-flotation experiments

The micro-flotation tests were carried out using a Hallimond tube. Air was used as the bubble source. When not used, galena feed was stored in a freezer (−14 °C), in a plastic bag which was purged with nitrogen to minimise sample oxidation. Using a ceramic mortar and pestle a small amount of feed material was ground shortly prior to the experiments. For each micro-flotation experiment around 3 g of galena feed sample were combined with 250 mL of a test solution (i.e., ~1.2 % solids). The test solution contained deionised water (DI) with NaCl concentration of 1, 10 or 100 mM, which also included 1 mM or 10 mM sodium ethyl xanthate. First, NaCl was dissolved in DI water, then the required amount of xanthate was added and mixed into the salt solution. In each experiment the pH was adjusted to 9 (±0.1). The pulp was transferred to the Hallimond tube and conditioned for 3 min. The tube was then aerated for 7 min with air at a flow rate of 60 mL/min, consistent with flotation times of 2–10 min used in other Hallimond tube micro-flotation studies (Wang et al., 2017; Nowosielska et al., 2022a, 2022b). From each micro-flotation experiment the concentrates and the tailings were recovered, filtered, and dried. To remove any salt residue from the samples, each fraction was rinsed using deionised (DI) water at least three times during filtration. The percentage (%) of galena recovery was calculated by dividing the mass of the froth concentrate by the combined mass of the froth concentrate and the tailings.

2.2.4. Ion competition at the galena and air bubble surface sites

The conventional DLVO theory does not include the effects of the pH-dependent interactions between particles and air bubbles. These effects can be included with a chemisorption (charge-regulation) model. A chemisorption model for galena was introduced in our previous work (Nowosielska et al., 2022a) and demonstrated that the charge regulation reactions can take place at a negative galena surface site X^-:

$$XH \overset{pK_{H_1}}{\Longleftrightarrow} X^- + H^+ \tag{1}$$

$$XNa \overset{pK_{Na}}{\Longleftrightarrow} X^- + Na^+ \tag{2}$$

and a neutral galena surface site X :

$$XH^+ \overset{pK_{H_2}}{\Longleftrightarrow} X + H^+ \tag{3}$$

$$XCl^- \overset{pK_{Cl}}{\Longleftrightarrow} X + Cl^- \tag{4}$$

This chemisorption model for galena is a “two-site/nonamphoteric” model, meaning that on the galena surface, only single-binding of ions will be taking place. Protons (H^+) are competing with sodium ions (Na^+) for the adsorption on the negative galena site as illustrated by Eqs. (1) and (2). On the neutral galena site, (Eqs. (3) and (4)), protons (H^+) compete with chloride anions (Cl^-) for direct surface adsorption.

In this work we introduce binding of the xanthate anion to the chemisorption model described by Eqs. (1)–(4), as an additional charge regulation reaction, Eq. (5), taking place on the neutral galena surface site X:

$$XR^- \overset{pK_R}{\Longleftrightarrow} X + R^- \tag{5}$$

where the term R^- denotes the xanthate anion. This has the consequence of leading to increased ion competition on the neutral galena sites, which now takes place between the protons (H^+), the chloride anions (Cl^-) and the xanthate anions (R^-). Previous investigations have described xanthate (R^-) adsorption in terms of a polar group attaching to the mineral surface (Leroy et al., 2012), while the nonpolar hydrophobic group is oriented outwards on the surface of the mineral, causing a stronger particle-air bubble attraction (Hu et al., 2020). Fig. 1 illustrates the competitive adsorption between all ions in the system on the galena surface sites, as described by Eqs. (1)–(5).

Similarly, there are charge regulation reactions arising at the air bubble surface sites, which can be represented as:

$$XH \overset{pK_H}{\Longleftrightarrow} X^- + H^+ \tag{6}$$

$$XH_2^+ \overset{pK_{HH}}{\Longleftrightarrow} XH + H^+ \tag{7}$$

$$XH - Cl^- \overset{pK_{HCl}}{\Longleftrightarrow} XH + Cl^- \tag{8}$$

Eqs. (6)–(8) are based on a model proposed by Leroy et al. (2012) with parameters fitted against air bubble zeta potentials measured by Yang et al. (2001). This air bubble model is an amphoteric “one-site/two pK” model which was applied in our previous work (Nowosielska et al., 2022a). Table 2 and Table 3 show the equilibrium constants (pK values) associated with the surface adsorption of each ion in the system. These were calculated by least-square fitting to the measured zeta potentials for the different NaCl concentrations. Here, the value (pK_R) representing xanthate binding is the new calculated parameter. All other values from tables 2 and 3 were taken from Nowosielska et al. (2022a).

We can calculate the total surface charge (σ_s) for any site according to:

$$\sigma_s = q_s N_s + \sum_i q_i \Gamma_i \tag{9}$$

where q_s is the charge of the dissociated site, N_s is the site density and q_i is the ionic charge (Parsons and Salis, 2015, 2019).

In Eq. (9), the total amount of bound charge (Γ_i) from any given ion (H^+, Na^+, Cl^-, xanthate) for the nonamphoteric case (i.e., galena chemisorption model) can be determined by:

$$\Gamma_i = \frac{N_s}{A_s}\left[\frac{a_i}{K_i}\right] \tag{10}$$

where the single binding of ion i (H^+, Na^+, Cl^-, xanthate) is represented by the binding constant K_i.

The term A_s in Eq. (10) represents the total association. For the nonamphoteric cases, it can be calculated according to the following:

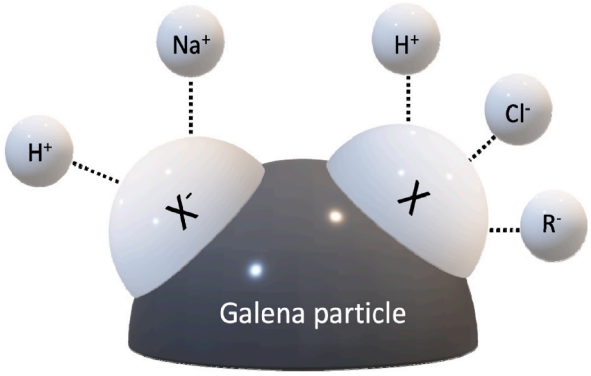

Fig. 1. An illustrative diagram describing the ion competition at the galena surface sites. Protons (H^+) and sodium (Na^+) cations compete to bind directly to a negatively charged galena surface site (X^-). At the neutral galena surface site (X), protons (H^+), chloride (Cl^-) anions and the xanthate (R^-) anions compete for the neutral galena surface site.

Table 2
Parameters used to fit the galena chemisorption model in NaCl/sodium ethyl xanthate solution (model parameters were calibrated using measured galena zeta potentials in 10 mM NaCl +1 mM sodium ethyl xanthate solution). Site densities and parameters H_1, H_2, Na and Cl were taken from Nowosielska et al. (2022a). The parameter for xanthate (R) is a new fitted parameter.

Parameter	Value
N_S negative (sites m^{-2})	1.519×10^{16}
N_S neutral (sites m^{-2})	2.765×10^{16}
pK_{H1}	5.265
pK_{H2}	2.393
pK_{Na}	−2.376
pK_{Cl}	7.911
pK_R	3.229

Table 3
Parameters used to fit the air bubble chemisorption model (Nowosielska et al., 2022a). These parameters were calibrated using the measured bubble zeta potentials (Yang et al., 2001), in 10 mM NaCl solution.

Parameter	Value
N_S (sites m^{-2})	4.676×10^{16}
pK_H	5.812
pK_{HH}	2.984
pK_{HCl}	1.962

$$A_s = 1 + \sum_i \frac{a_i}{K_i} \tag{11}$$

In the case of the amphoteric ion competition (i.e., air bubble chemisorption model), the total amount of bound charge (Γ_i) can be expressed as:

$$\Gamma_i = \frac{N_s}{A_{ss}}\left[\frac{a_i}{K_i} + \sum_j a_i a_j \left(\frac{1}{K_i K_{ij}} + \frac{1}{K_j K_{ji}}\right)\right] \tag{12}$$

The double binding terms K_{ij} and K_{ji} describe the adsorption of ion i to a site where ion j has attached prior, and the adsorption of ion j to a site where ion i is already bound, respectively.

For the cases involving the amphoteric ion competition, Eq. (11) can be re-written as:

$$A_{ss} = 1 + \sum_i \frac{a_i}{K_i}\left(1 + \sum_j \frac{a_j}{K_{ij}}\right) \tag{13}$$

The term a_i in Eq. (12) and Eq. (13) correspond to the "partial ion activity" for a given concentration (Parsons and Salis, 2019), defined as:

$$a_i = c_i^{bulk} e^{-q_i \psi_0 / kT} \tag{14}$$

where c_i^{bulk} is the bulk concentration of ion i (H^+, Na^+, Cl^- or xanthate) in solution, ψ_0 is the surface electrostatic potential, k is the Boltzmann constant (1.3806×10^{-23} J/K) and T is the temperature (298 K).

2.2.5. Total interaction free energy

The total free interaction energy, technically a grand potential (Tadesse and Parsons, 2023), between any two objects at some distance apart can be attributed to the various individual attractive and repulsive interaction components. In this work, the total interaction energy (F_{tot}) is represented as four individual contributions:

$$F_{tot} = F_{el} + F_{en} + F_{vdW} + F_{chem} \tag{15}$$

The first term, F_{el}, illustrates the direct electrostatic energy, according to the following:

$$F_{el} = \frac{1}{2}\int d^3 r D(r) E(r) \tag{16}$$

The term E(r) represents the electric field taken as $E(r) = -\nabla\psi(r)$, where $\psi(r)$ is the electrostatic potential. The term D(r) from Eq. (16) is the electric displacement: $D(r) = \varepsilon_0 \varepsilon E(r)$, where ε_0 is the permittivity of the vacuum and ε is the dielectric constant of water (Parsons and Ninham, 2011).

The second term, F_{en}, in Eq. (15) originates from the ideal entropy of physiosorbed ions at the surface, and can be determined using the adsorbed ions concentration profiles $c_i(z)$:

$$F_{en} = kT \sum_i \int_0^L dz \left\{ c_i(z) \ln \frac{c_i(z)}{c_{i0}} - c_i(z) + c_{i0} \right\} \tag{17}$$

where c_{i0} is the concentration of ion i in the bulk (Parsons and Ninham, 2012).

The non-electrostatic van der Waals interactions represented by the term F_{vdW} can be calculated by:

$$F_{vdW} = \frac{-A_{132}}{12\pi L^2} \tag{18}$$

where A_{132} is the Hamaker constant which characterises the interaction between sphere 1 (galena particle) and sphere 2 (air bubble) immersed in aqueous medium 3 (aqueous solution). The Hamaker constant value characterising the galena-air bubble interaction in water used in this study was 2.7741×10^{-21} J or 0.67392 kT. This value was first calculated and presented in Nowosielska et al. (2022b), using dielectric data for galena from Bergström (1997) and for water from Fiedler et al. (2020). Any effects of xanthate and other ions on the Hamaker constant and the van der Waals interactions are expected to be negligible and were not included in the investigation.

Lastly, the term F_{chem} from Eq. (15) represents the chemisorption free energy. Due to its complexity, a more detailed description of this energy contribution can be found in the works of Parsons and Salis, 2015, 2019.

The total interaction energy (grand potential) from Eq. (15) arises due to ion adsorption at the surface in response to the electrostatic potential $\psi(z)$, with each ion forming a concentration profile $c_i(z)$. If each ion is in equilibrium with the bulk solution, its concentration profile $c_i(z)$ will follow a Boltzmann distribution, according to:

$$c_i(z) = c_{i\infty} \exp\left(-\frac{z_i e \psi(z)}{kT}\right) \tag{19}$$

where k is the Boltzmann constant, T is the temperature and $c_{i\infty}$ is the concentration of all the ions in the bulk solution.

The term $\psi(z)$ from Eq. (19), which represents the electrostatic potential can be determined by applying the Poisson equation:

$$\frac{d^2}{dz^2}\psi(z) = -\frac{e}{\varepsilon\varepsilon_0}\sum_i z_i c_{i\infty} \exp\left(-\frac{z_i e \psi(z)}{kT}\right) \tag{20}$$

where e is the elementary charge and z_i is the ion valency. The terms ε and ε_0 are the dielectric constant of the medium and the permittivity of free space, respectively. In this study, the boundary conditions for the Poisson equation (Eq. 20) are defined by the charge regulation model from Eq. (9), as follows:

$$\left(\frac{d\psi}{dz}\right)_{surface} = \frac{-\sigma}{\varepsilon\varepsilon_0} \tag{21}$$

Finally, computing $c_i(z)$ from Eq. (19) and $\psi(z)$ from Eq. (20) simultaneously, forms what is known as the nonlinear Poisson-Boltzmann (PB) model. This model was then solved by finite element methods using the FEniCS software (Alnæ et al., 2015). Lastly, the Derjaguin approximation (Derjaguin, 1934) was used to convert the flat-plane interaction energy (F_{tot}) from Eq. (15) into an energy

representing the interactions between two spherical objects (i.e., galena particle and an air bubble). For a more in-depth description of the calculation sequence implemented in this study the authors direct the reader to the following works (Nowosielska et al., 2022a, 2022b).

3. Results and discussion

3.1. Contact angle

When determining the optimum conditions for the highest mineral recovery, the wettability of a particle surface is an important property to consider. For a mineral flotation system, where a particle (solid), water (liquid) and an air bubble (gas) co-exist at a three-phase contact line, a contact angle is often used to characterise the wettability of the mineral particle surface.

Young (1805), was the first to recognise a connection between the contact angle and surface tension. He suggested that the contact angle can be determined by the free energies of a solid-gas, a liquid-gas and a solid-liquid interface as follows:

$$\cos\theta = \frac{\gamma_{SG} - \gamma_{SL}}{\gamma_{LG}} \quad (22)$$

where θ is the contact angle and γ_{SG}, γ_{SL} and γ_{LG} are the free energies (nNm^{-1}) of the solid-gas, solid-liquid, and liquid-gas interfaces, respectively (Young, 1805).

In this study, the contact angle measurements were conducted using liquids containing 1, 10 or 100 mM NaCl with and without the addition of xanthate, at pH 9 (±0.1), and are shown in Fig. 2. Our measured water contact angle (i.e., without any other reagents in the system) on the galena surface was 51°, which is compatible with the water contact angles (48–52°) measured by other researchers (Chen et al., 2014).

As seen in Fig. 2, for the 'NaCl only' solutions (i.e., with no xanthate), the contact angles of galena increased with the increase of NaCl concentration, from ~57° in 1 mM NaCl solution to ~70° in 100 mM NaCl solution. Several studies reported that when an inorganic salt, such as NaCl, is dissolved in water, the surface tension of water will increase (Ozdemir et al., 2009; Matubayasi et al., 2011; Pegram and Records, 2007), indicating a negative ion adsorption at the liquid-gas interface. Liquids with a higher surface tension would give rise to larger contact angles, because the molecules of the liquid display a stronger attraction towards each other than to the molecules on the solid surface.

Table 4 illustrates the relationship between the surface tension and the concentration of NaCl in solution, taken from Ozdemir et al. (2009).

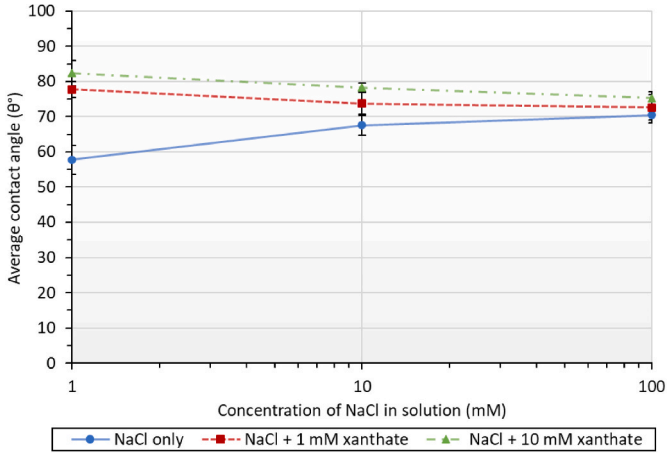

Fig. 2. Contact angles measured on a fresh galena surface using NaCl solutions (1, 10 and 100 mM) at, pH 9 (±0.1), with or without 1 mM or 10 mM xanthate. The galena contact angles measured in 1 and 10 mM 'xanthate only' solutions (80.5° and 87.7°, respectively) are also included. Here, the error bars represent the 95% confidence interval of the distribution.

From the results in Fig. 2 and Table 4, however, the increasing contact angles cannot be explained in terms of the increases in surface tension, since the effect is too small to account for the magnitude of the change in contact angle. More likely, the increasing contact angles are due to the decrease in galena surface potential (i.e., decreasing galena zeta potentials) resulting from the increasing NaCl concentration in solution (Churaev and Sobolev, 1995; Chau et al., 2009), as illustrated in Fig. 3. Such solutions will show a limited tendency towards surface wetting. Jeldres et al. (2016) showed that the addition of NaCl reduces surface hydration, subsequently, improving the floatability of galena.

The contact angles of galena increased with the addition of xanthate in the absence of NaCl. For example, the water contact angle of galena was 51°, which increased to 80.5° in the presence of 1 mM xanthate and to 87.7° in the presence of 10 mM xanthate. The increase in measured contact angles for solutions containing xanthate and no NaCl indicates a positive adsorption of xanthate on the galena surface, resulting in the surface becoming more hydrophobic, thus increasing galena floatability (Prestidge and Ralston, 1995, 1996; Fosu et al., 2015; Abaka-Wood et al., 2017). If the measured contact angle increases, it is an indication that the area of contact between the mineral particle and the air bubble also increases, and the probability of particle-bubble detachment during flotation will be much lower.

It has been reported that the addition of xanthate to water with no NaCl present decreases the surface tension due to the molecules of the liquid displaying a stronger attraction towards the solid surface than to each other. Leelamanie and Karube (2013) explained that a liquid with a lower surface tension will show a stronger attraction towards the solid surface, and this will potentially result in a higher number of xanthate ions adsorbing on the galena surface and increasing galena recoveries. According to Wang et al. (2019), the surface tension will keep decreasing with an increasing xanthate concentration to a point when xanthate adsorbed at the liquid-gas interface will reach a stable value at a critical micelle concentration (CMC), at which point the curve will plateau.

When looking at the contact angles of galena in 'NaCl/xanthate' solutions, it is evident that these contact angles are smaller than the ones measured in 'xanthate only' solutions with no NaCl. As the concentration of NaCl increases from 1 to 100 mM, the contact angles become even smaller. The measured contact angles with NaCl +1 mM xanthate ranged from ~78° (1 mM NaCl) to ~72° in 100 mM NaCl solution. The contact angles in NaCl +10 mM xanthate ranged from ~82° (1 mM NaCl) to ~75° in 100 mM NaCl. The lower galena contact angles with increasing NaCl concentrations in the NaCl/xanthate solutions, shown in Fig. 2, suggest that NaCl depresses the adsorption of xanthate on the surface of galena, leading to the galena surface becoming less hydrophobic. The decrease in galena surface hydrophobicity indicated by these lower contact angles is most likely due to the competitive adsorption of salt ions and xanthate. Atkin et al. (2003) reported that increasing salt concentration in solution provides more co-ions to compete with the surfactant (xanthate) for the available surface sites, consequently reducing the degree of adsorption of xanthate.

In the presence of NaCl, xanthate adsorption on the sulfide mineral surface results in a multilayer formation. The direct chemisorption of xanthate creates the first layer on the surface, followed by the adsorption of metal ions/xanthate complexes in the top layer. Higher wettability of the galena surface, indicated by the lower measured contact angles in

Table 4
Average equilibrium surface tension as a function of NaCl concentration in solution at 23 °C (Ozdemir et al., 2009).

Concentration (M)	Surface Tension (mN/m)	Standard Deviation (mN/m)
0.00	72.72	0.03
0.25	73.03	0.09
0.50	73.46	0.03
1.00	74.05	0.05

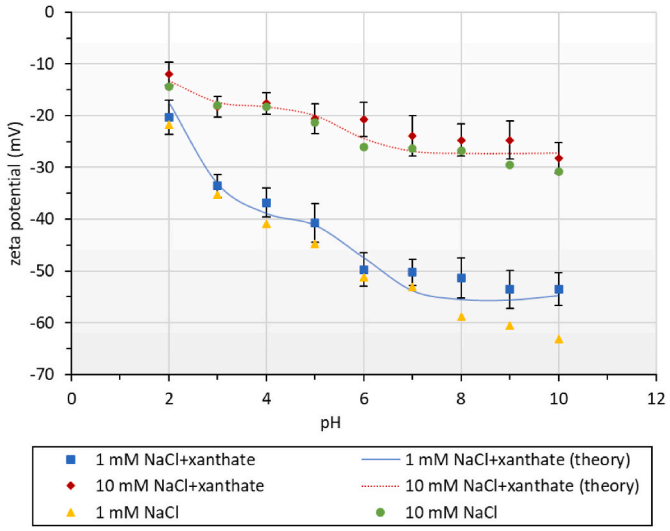

Fig. 3. The measured zeta potentials of galena as a function of solution pH. These measurements were performed using 1 and 10 mM NaCl +1 mM xanthate. The calculated values are represented by lines (solid or broken). These were obtained using the galena chemisorption model. The measured zeta potentials without xanthate (Nowosielska et al., 2022a) are also shown (i.e., 1 and 10 mM NaCl). Error bars represent the 95% confidence interval of the distribution.

NaCl + xanthate solutions in Fig. 2, implies that there is a more stable liquid layer on the mineral surface, therefore, the time necessary to form particle-bubble attachments will increase. The lower measured contact angles in NaCl + xanthate solutions could be an indication that the species in the top layer may adsorb with their polar groups oriented more towards the liquid phase (Pan and Yoon, 2009).

3.2. Zeta potential and xanthate adsorption

The measured and calculated zeta potentials for galena conditioned in 1 and 10 mM NaCl +1 mM xanthate, are presented in Fig. 3. Here we have also included the zeta potentials of galena which were measured using 1 and 10 mM NaCl as background electrolyte solutions, in the absence of xanthate. These were taken from Nowosielska et al. (2022a).

As the solution pH increased from 2 to 10, the zeta potential values of galena in 1 and 10 mM NaCl + xanthate solutions decreased from −21 to −53 mV and from −13 to −28 mV, respectively, with the isoelectric point (IEP) around pH < 1. Several studies reported that the (IEP) of galena is found at pH < 1, while others indicated that it occurs somewhere between pH 2 and pH 8 (Fairthorne et al., 1998; Fullston et al., 1999; Pugh and Forsberg, 1988), with the differences mainly attributed to sulfide mineral oxidation (Huo et al., 2019). In this current study, a galena (IEP) at pH < 1 indicates a non-oxidised (Wang et al., 2017; Pugh and Forsberg, 1988) negatively charged galena surface with the zeta potential values close to those of elemental sulfur (S^0).

According to Fig. 3, the zeta potentials of galena became more negative at the lower NaCl concentrations. The more negative zeta potentials at the lower NaCl concentrations can also inhibit galena-air bubble attachments, decreasing flotation efficiency (October et al., 2021).

As the NaCl concentration was increased, the ionic diffuse layers compress (Wang and Peng, 2014), and cause the zeta potentials to become less negative. An increase in NaCl concentration in the bulk solution will increase the number of counter-ions in the Stern layer, leading to an increased attraction/decreased repulsion, as well as promoting particle aggregation (October et al., 2021).

In the presence of xanthate, minimal or no change in the zeta potentials was observed for galena in 'NaCl only' solutions (i.e., no xanthate) compared to the solutions of the same NaCl concentration with the addition of xanthate. In fact, the addition of xanthate made the zeta potentials slightly less negative for both NaCl salt solutions, displaying a trend in zeta potential changes usually associated with an increase in the solution ionic strength. The fact that the galena (IEP) does not shift as a result of xanthate addition to the system indicates that, due to the competitive ion adsorption at the surface sites, the chemisorption of xanthate is weak. The chemisorption model for galena Eqs. (1)–(5) indicates that galena surface charge is mainly controlled by the chloride anions ($pK_{Cl} = 7.911$) in the system and to a lesser extent by the xanthate anions ($pK_R = 3.229$). Therefore, we speculate that these slightly less negative galena zeta potentials for the NaCl/xanthate solutions are most likely attributed to the competitive adsorption of the neutral lead dixanthate (PbR_2) complex and Cl^- anions on the neutral galena binding site (X), resulting in a reduced Cl^- adsorption with a corresponding reduction in the magnitude of the negative zeta potential.

3.3. Micro-flotation

Fig. 4 shows the outcome of the micro-flotation experiments on galena in solutions with different NaCl concentrations, at pH 9 (±0.1), with/without xanthate addition.

Fig. 4 shows increasing galena recoveries for higher NaCl and xanthate concentrations. These higher galena recoveries can be attributed to compression of the ionic diffuse layers leading to a higher degree of particle aggregation, caused by weaker repulsive interactions (Wang and Peng, 2014). Additionally, an increasing NaCl concentration in solution has been shown to inhibit bubble coalescence (Craig et al., 1993a, 1993b), with the reduction in bubble size likely responsible for promoting a more stable froth phase (Castro et al., 2013; Quinn et al., 2014). Consequently, the addition of NaCl will increase the number of air bubbles in the system which are smaller in size, increasing the particle-bubble collision and attachment efficiencies (Wu et al., 2016; Quinn et al., 2014; Klassen and Mokrousov, 1963), and resulting in higher mineral recoveries.

In Fig. 4, the recovery of galena as a function of NaCl concentration for solutions containing 1 mM xanthate, increased from ~79% to ~90%. Similarly, the recovery of galena using solutions containing 10 mM xanthate also increased from ~83% to ~95%. Considering that the adsorption of xanthate on the surface of galena is limited by a stronger chemisorption of the chloride ions in the system, we expected to see lower galena recoveries with increasing NaCl/xanthate solution concentrations. However, the results in Fig. 4 demonstrate a slightly

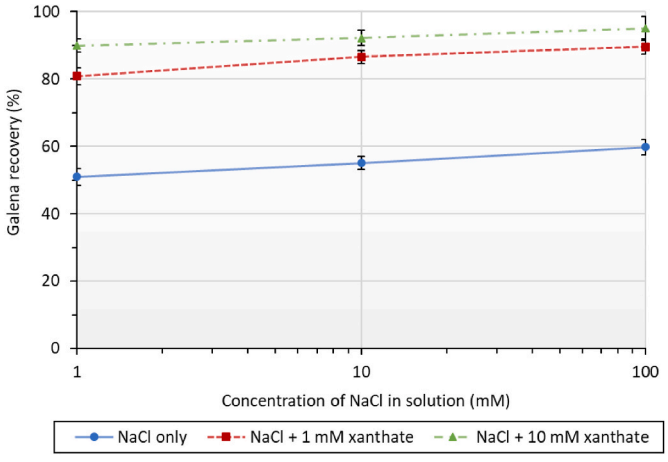

Fig. 4. Recovery of galena as a function of the NaCl concentration in solution, at pH 9 (±0.1), after 7 min of flotation time, with/without the addition of xanthate. Here we have also included the recoveries of galena in 1, 10 and 100 mM 'NaCl only' solutions, taken from Nowosielska et al. (Nowosielska et al., 2022a). The error bars indicate the 95% confidence interval of the distribution.

different outcome, implying that the competitive chemisorption between xanthate and chloride in the system is not the only mechanism responsible for the amount of xanthate adsorbed on galena. We speculate that there could be two independent mechanisms which contribute to the adsorption of xanthate in NaCl solutions. Firstly, xanthate adsorption can take place via a direct chemisorption (although largely suppressed by the chloride anions in the system), where it forms surface complexes chemisorbed to the neutral galena site. Secondly, when the surface of galena is oxidised, dissolved metal ions can form complexes with xanthate and attach on the galena surface as hydrophobic metal xanthate salts.

According to the Pourbaix diagrams in Fig. 5, galena reacts with oxygen to create lead sulfate ($PbSO_4$) complexes:

$$PbS_{(s)} + 2O_{2\,(g)} \rightarrow PbSO_{4\,(s)} \quad (23)$$

With the system open to air, carbon dioxide will also be present, and the galena surfaces will start to form lead carbonate ($PbCO_3$) at the expense of lead sulfate:

$$PbSO_{4\,(s)} + CO_3^{2-} \rightarrow PbCO_{3\,(s)} + SO_4^{2-} \quad (24)$$

In addition, formation of the lead-chloride complexes in a chloride system will cause a reduction of the corrosion product film on the galena surface (Woods et al., 1987):

$$Pb^{2+} + Cl^- \rightarrow PbCl^+ \quad (25)$$

The flotation tests using a xanthate collector are usually carried out in solutions with pH 8–9.5. In this pH region, lead dixanthate (PbR_2) is a more stable complex than lead sulfate, lead carbonate or lead chloride. This lead dixanthate complex formation takes place via the following electrochemical reactions:

$$PbS + 2R^- \rightarrow PbR_2 + S^0 + 2e^- \text{ (Anodic)} \quad (26)$$

$$H_2O + 0.5\,O_2 + 2e^- \rightarrow 2OH^- \text{ (Cathodic)} \quad (27)$$

The results from a study conducted by Zha et al. (2020) indicated

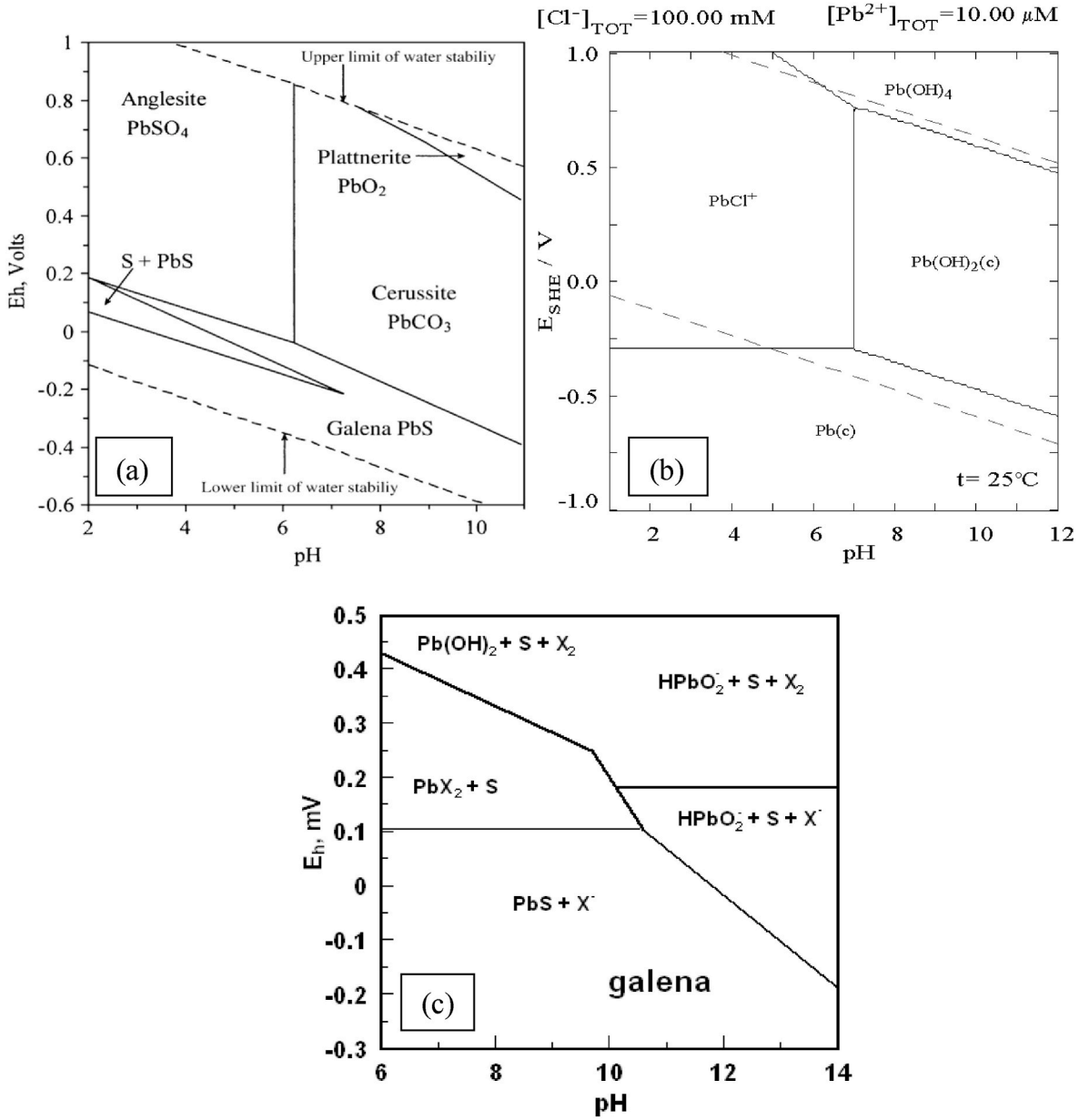

Fig. 5. Pourbaix diagrams for **(a)** lead minerals at 298 K and 1 bar (Krauskopf and Bird, 1994); **(b)** lead in chloride (0.1 M) media (Krauskopf and Bird, 1994), and **(c)** galena and ethyl xanthate (10^{-4} M). Here X^- represents ethyl xanthate (Puigdomenech, 2004).

that in higher NaCl concentrations, the passive layer on the galena surface deteriorates and becomes more susceptible to corrosion. The authors observed that due to the higher NaCl concentrations, the open circuit potential (OCP) value of galena is significantly reduced. Subsequently, a higher number of Pb^{2+} ions is released into the bulk solution where they are available to form complexes with the xanthate ions. The Pb^{2+} ion bulk concentration will be high due to their weaker direct chemisorption on the galena surface sites. Consequently, the formation of lead dixanthate (PbR_2), a hydrophobic product which attaches to the sulfur sites in the galena lattice will take place, as illustrated in Fig. 6.

Our micro-flotation experiment results in Fig. 4 showed higher galena recoveries for higher NaCl + xanthate concentrations in solution. If the direct chemisorption between the salt ions and xanthate was the only parameter controlling/limiting xanthate adsorption on the surface of galena, lower galena recoveries would be expected. However, because galena recoveries increase, it is speculated that these increases may be attributed to xanthate ions forming complexes with the surface dissolved Pb^{2+} ions, an adsorption mechanism which is facilitated by Cl^- ions, weakening the passive layer on the galena surface.

3.4. Total interaction free energy

The galena-air bubble total interaction free energy curves as a function of separation distance are shown in Fig. 7. These curves represent the galena-air bubble interaction in NaCl solutions (1, 10 and 100 mM) with and without xanthate (1 and 10 mM), at pH 9.

The energy profiles for 1 mM NaCl indicate the highest energy barriers of $\sim 12 \times 10^{-16}$ J, 7×10^{-16} J and 3×10^{-16} J for 'NaCl only', and with the addition of 1 and 10 mM xanthate, respectively. As seen in Fig. 7, the addition of xanthate decreases the height of the energy barrier, implying that significantly less kinetic energy will be required to form particle-bubble aggregates. It is also interesting to note that the profiles for 1 mM NaCl and 1 mM NaCl +1 mM xanthate profiles indicate a secondary minimum at >25 nm. This secondary minimum represents a metastable galena-bubble equilibrium where a weak attraction will dominate the interactions. However, based on the profiles in Fig. 7, this attraction was not sufficient to maintain a stable galena-air bubble aggregation, and would eventually cause them to redisperse.

The energy profiles for interactions in 10 mM NaCl also indicate repulsive interactions, however the energy barriers are significantly smaller, ranging from $\sim 2 \times 10^{-16}$ J in 'NaCl only' to $\sim 1.8 \times 10^{-16}$ J and $\sim 1 \times 10^{-16}$ J with the addition of 1 and 10 mM xanthate, respectively. In fact, there are minimal differences in the energy profiles for 10 mM NaCl and 10 mM NaCl +1 mM xanthate, suggesting that the addition of

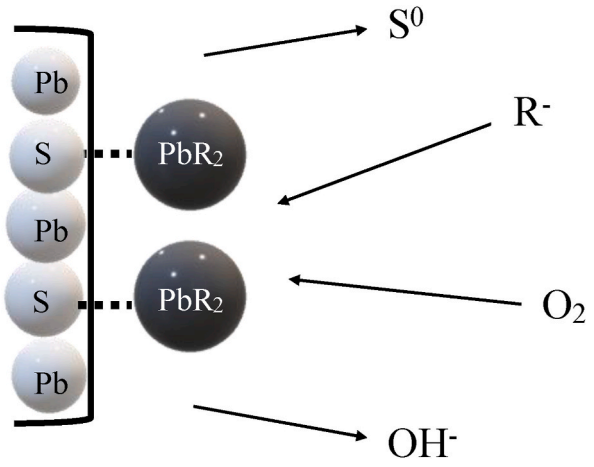

Fig. 6. A schematic representation of the electrochemical theory of xanthate adsorption on a galena surface. Here, the lattice sulfide ion gets oxidised to sulfur.

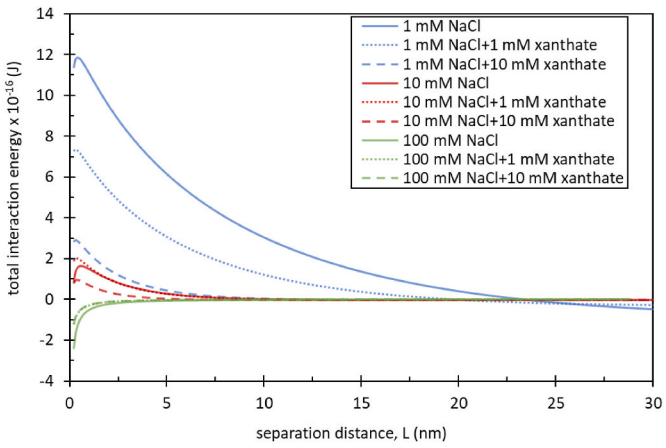

Fig. 7. The galena-air bubble total interaction free energies versus the distance of separation, at pH 9, in varying NaCl concentrations with and without an addition of sodium ethyl xanthate. The particle and air bubble diameters used in the calculations were 80 μm and 2000 μm, respectively.

1 mM xanthate is insignificant for the galena-air bubble interactions in 10 mM NaCl solution. In contrast, the addition of 10 mM xanthate lowers the galena-bubble repulsion, as illustrated in Fig. 7.

In 100 mM NaCl solution, the total interaction energy between galena and an air bubble is always attractive. This attraction arises from the screening of the particle and bubble ionic diffuse layers at higher ionic concentrations, such that the total interaction becomes controlled by the attractive van der Waals forces. Based on the results in Fig. 7, it can be concluded that xanthate addition has no significant effect on the galena-air bubble interactions in 100 mM NaCl solution. These trends are consistent with studies found in the literature that documented the adsorption competition between xanthate and other inorganic salt ions on the mineral surface (October et al., 2021; Fuerstenau et al., 2003; Laskowski, 2013).

4. Conclusion

This study focused on the effects of NaCl on galena flotation in the presence of xanthate. It was demonstrated that galena recovery improves with an increase in NaCl and xanthate concentrations.

The charge regulation effect of xanthate on our previously identified galena chemisorption model was investigated. Our results indicated that xanthate anions have weaker chemisorption than chloride anions, therefore, we hypothesize that the charge on the galena surface could be predominantly controlled by the stronger adsorption of chloride than xanthate. Based on these outcomes, we proposed that there are two separate adsorption mechanisms involved in the adsorption of xanthate on the surface of galena in NaCl salt solutions, one involving direct chemisorption, and a second, due to metal ions complexing with xanthate in the bulk solution.

A chemisorption (charge regulation) model used with DLVO theory showed that repulsive forces dominated at the lowest NaCl concentrations showed attractive interactions, mainly due to the more dominant van der Waals forces. As the NaCl concentration increases, the effects of xanthate on the total interaction free energy becomes insignificant. The total interaction free energy model predictions appeared in accordance with the micro-flotation recovery results, which suggests that these can effectively estimate the flotation behaviour of galena.

Further research, especially focusing on the proposed second adsorption mechanism, is necessary to fully understand the particle-bubble interactions under the studied system conditions. Additionally, the effects of xanthate on the Hamaker constant and the van der Waals interactions will need to be investigated in order to better understand xanthate effect on galena during NaCl flotation.

CRediT authorship contribution statement

Anna M. Nowosielska: Writing – review & editing, Writing – original draft, Methodology, Investigation, Formal analysis, Data curation, Conceptualization. **Aleksandar N. Nikoloski:** Writing – review & editing, Validation, Supervision, Resources, Methodology, Funding acquisition. **Drew F. Parsons:** Writing – review & editing, Supervision, Software, Methodology.

Declaration of competing interest

The authors declare that they have no known competing financial interests or personal relationships that could have appeared to influence the work reported in this paper.

Data availability

Data will be made available on request.

Acknowledgements

This work was performed independently, that is from general academic support from the universities, not a specific funded grant.

References

Abaka-Wood, G.B., Addai-Mensah, J., Skinner, W., 2017. A study of flotation characteristics of monazite, hematite and quartz using anionic collectors. Int. J. Miner. Process. 158, 55–62.
Alnæs, M., Blechta, J., Hake, J., Johansson, A., Kehlet, B., Logg, A., Richardson, C., Ring, J., Rognes, M.E., Wells, G.N., 2015. The FEniCS project version 1.5. Archive of Numerical Software 3 (100).
Atkin, R., Craig, V.S.J., Wanless, E.J., Biggs, S., 2003. The influence of chain length and electrolyte on the adsorption kinetics of cationic surfactants at the silica-aqueous solution interface. J. Colloid Interface Sci. 266, 236–244.
Bergström, L., 1997. Hamaker constants of inorganic materials. Adv. Colloid Interface Sci. 70.
Berry, J.D., Neeson, M.J., Dagastine, D.Y., Chan, C., Tabor, R.F., 2015. Measurement of surface and interfacial tension using pendant drop tensiometry. J. Colloid Interface Sci. 454, 226–237.
Boujounoui, K., Abidi, A., Bacaoui, A., Amari, K.E., Yaacoubi, A., 2015. The influence of water quality on the flotation performance of complex sulfide ores: case study at Hajar Mine, Morocco. J. S. Afr. Inst. Min. Metall 115, 1243–1251.
Buckley, A.N., Woods, R., 1994. On the characterization of sulfur species on sulfide mineral surfaces by XPS and Raman spectroscopy. J. Electroanal. Chem. 370, 295–296.
Castro, S., Miranda, C., Toledo, P., Laskowski, J.S., 2013. Effect of frothers on bubble coalescence and foaming in electrolyte solutions and seawater. Int. J. Miner. Process. 124, 8–14.
Chang, Z., Chen, X., Peng, Y., 2018. The adsorption behaviour of surfactants on mineral surfaces in the presence of electrolytes – a critical review. Miner. Eng. 121, 66–76.
Chau, T.T., Bruckard, W.J., Koh, P.T.L., Nguyen, A.V., 2009. A review of factors that affect contact angle and implications for flotation practice. Adv. Colloid Interface Sci. 150 (2), 106–115.
Chen, J., Long, X., Chen, Y., 2014. Comparison of the multilayer water adsorption on the hydrophobic galena (PbS) and hydrophilic pyrite (FeS_2) surfaces: a DFT study. J. Phys. Chem. C 118, 11657–11665.
Churaev, N.V., Sobolev, V.D., 1995. Prediction of contact angles on the basis of the Frumkin-Derjaguin approach. Adv. Colloid Interface Sci. 61, 1–16.
Craig, V.S.J., Ninham, B.W., Pashley, R.M., 1993a. The effect of electrolytes on bubble coalescence in water. J. Phys. Chem. 97 (39), 10192–10197.
Craig, V.S.J., Ninham, B.W., Pashley, R.M., 1993b. Effect of electrolytes on bubble coalescence. Nature 364 (6435), 317–319.
Derjaguin, B.V., 1934. Untersuchungen über die Reibung und Adhäsion, IV. Kolloid Z. 69.
Dobby, G.S., Finch, J.A., 1986. Particle collection in columns-Gas rate and bubble size effects. Can. Metall. Q. 27, 85–90.
Elizondo-Alvarez, M.A., Flores-Alvarez, J.M., Davila-Pulido, G.I., Uribe-Salas, A., 2017. Interaction mechanism between galena and calcium and sulfate ions. Miner. Eng. 111, 116–123.
Fairthorne, G., Brinen, J.S., Fornasiero, D., Nagaraj, D.R., Ralston, J., 1998. Spectroscopic and Electrokinetic study of the adsorption of butyl ethoxy carbonyl thiourea on chalcopyrite. Int. J. Miner. Process. 54, 147–163.
Fiedler, J., Boström, M., Persson, C., Brevik, I., Corkery, R., Buhmann, S.Y., Parsons, D.F., 2020. Full-spectrum high-resolution modelling of the dielectric function of water. J. Phys. Chem. B 124.
Fornasiero, D., Li, F., Ralston, J., 1994. Oxidation of galena II. Electrokinetic study. J. Colloid Interface Sci. 164, 345–354.
Fosu, S., Skinner, W., Zanin, M., 2015. Detachment of coarse composite sphalerite particles from bubbles in flotation: influence of xanthate collector type and concentration. Miner. Eng. 71, 73–84.
Fuerstenau, D.W., Rosenbaum, J.M., Laskowski, J., 1983. Effect of surface functional groups on the flotation of coal. Colloid. Surface. 8 (2), 153–173.
Fuerstenau, M.C., Somasundaran, P., 2003. Flotation. In: Fuerstenau, M.C., Han, K., K (Eds.), Principles of Mineral Processing Society for Mining, Metallurgy and Exploration (SME) (Littleton, Colorado).
Fullston, D., Fornasiero, D., Ralston, J., 1999. Zeta potential study of the oxidation of copper sulfide minerals. Colloids Surf. A Physicochem. Eng. Asp. 146 (1–3), 113–121.
Grano, S.R., Wong, P.L., Skinner, W., Johnson, N.W., Ralston, J., 1995. Detection and control of calcium sulfate precipitation in the lead circuit of the hilton concentrator of mount isa mines limited, Australia. In: Proceedings of the XIX International Mineral Processing Congress. SME, pp. 171–179. Littleton, Colorado.
Grano, S.R., Prestidge, C.A., Ralston, J., 1997. Solution interaction of ethyl xanthate and sulphite and its effect on galena flotation and xanthate adsorption. Int. J. Miner. Process. 52, 161–186.
Han, K.N., Healy, T.W., Fuerstenau, D.W., 1973. The mechanism of adsorption of fatty acids and other surfactant at the oxide-water interface. J. Colloid Interface Sci. 44, 407–414.
Han, Y., Han, S., Kim, B., Yang, J., Choi, J., Kim, K., You, K., Kim, H., 2019. Flotation separation of quartz from apatite and surface forces in bubble-particle interactions: role of pH and cationic collector contents. J. Ind. Eng. Chem. 70, 107–115.
Hancer, M., Celik, M.S., Miller, J.D., 2001. The significance of interfacial water structure in soluble salt flotation systems. J. Colloid Interface Sci. 235, 150–161.
Harvey, P.A., Nguyen, A.V., Evans, G.M., 2002. Influence of electrical double-layer interaction in coal flotation. J. Colloid Interface Sci. 250, 337–343.
Hu, Y., Wu, M., Liu, R., Sun, W., 2020. A review on the electrochemistry of galena flotation. Miner. Eng. 150, 106272.
Huo, W., Zhang, X., Gan, K., Chen, Y., Xu, J., Yang, J., 2019. Effect of zeta potential on properties of foamed colloidal suspension. J. Eur. Ceram. Soc. 39, 574–583.
Ikumapayi, F., Makitalo, M., Johansson, B., Rao, K.H., 2012. Recycling of process water in sulphide flotation: effect of calcium and sulphate ions on flotation of galena. Miner. Eng. 39, 77–88.
Jeldres, R.I., Forbes, L., Cisternas, L.A., 2016. Effect of seawater on sulfide ore flotation: a review. Miner. Process. Extr. Metall. Rev. 37 (6), 369–384.
Jordens, A., Cheng, Y.P., Walters, K.E., 2013. A review of the beneficiation of rare earth element bearing minerals. Miner. Eng. 41, 97–114.
Klassen, V.I., Mokrousov, V.A., 1963. An Introduction to the Theory of Flotation. Butterworths, London.
Krauskopf, K.B., Bird, D.K., 1994. Introduction to Geochemistry. McGraw-Hill International Editions, New York, USA, 3rd ed.
Laskowski, J.S., 2013. From amine molecules adsorption to amine precipitate transport by bubbles: a potash ore flotation mechanism. Miner. Eng. 45, 170–179.
Laskowski, J.S., Castro, S., 2015. Flotation in highly concentrated electrolyte solutions. Int. J. Miner. Process. 144, 50–55.
Laskowski, J., Iskra, J., 1970. Role of capillary effect in bubble-particle collision in flotation. Trans. Inst. Min. Metall. 79, C1–C6.
Leelamanie, D.A.L., Karube, J., 2013. Soil-water contact angle as affected by the aqueous electrolyte concentration. Soil Sci. Plant Nutr. 59, 501–508.
Leroy, P., Jougnot, D., Revil, A., Lassin, A., Azaroual, M., 2012. A double-layer model of the gas bubble/water interface. J. Colloid Interface Sci. 388, 243–256.
Liu, W., Moran, C., Vink, S., 2013. A review of the effect of water quality on flotation. Miner. Eng. 53, 91–100.
Lucay, F., Cisternas, L.A., Galves, E.D., Lopez-Valdivieso, A., 2015. Study of the natural floatability of molybdenite fines in saline solutions. Effects of gypsum precipitation. Minerals and Metallurgical Processing Journal 32, 203–208.
Marrucci, G., Nicodemo, L., 1967. Coalescence of gas bubbles in aqueous solutions in inorganic electrolytes. Chem. Eng. Sci. 22 (9), 1257–1265.
Matubayasi, N., Takayama, K., Ito, R., Takata, R., 2011. Thermodynamic quantities of surface formation of aqueous electrolyte solutions X. Aqueous solutions of 2:1 valence type salts. J. Colloid Interface Sci. 356, 713–717.
Nguyen, A.V., Schulze, H.J., 2004. Colloidal Science of Flotation. Marcel Dekker Inc., New York.
Nowosielska, A.M., Nikoloski, A.N., Parsons, D.F., 2022a. A theoretical and experimental study of the effects of NaCl and the competitive chemisorption of ions at the surface sites in the context of galena flotation. Miner. Eng. 182, 107540.
Nowosielska, A.M., Nikoloski, A.N., Parsons, D.F., 2022b. Interactions between coarse and fine galena and quartz particles and their implications for flotation in NaCl solutions. Miner. Eng. 183, 107591.
October, L.L., Manono, M.S., Wiese, J.G., Schreithofer, N., Corin, K.C., 2021. Fundamental and flotation techniques assessing the effect of water quality on bubble-particle attachment of chalcopyrite and galena. Miner. Eng. 167, 106880.
Ozdemir, O., Karakashev, S.I., Nguyen, A.V., Miller, J.D., 2009. Adsorption and surface tension analysis of concentrated alkali halide brine solutions. Miner. Eng. 22, 263–271.
Pan, L., Yoon, R.H., 2009. Hydrophobic forces in the wetting films of water formed on xanthate-coated gold surfaces. Faraday Discuss 146, 325–340.
Parsons, D.F., Ninham, B.W., 2011. Surface charge reversal and hydration forces explained by ionic dispersion forces and surface hydration. Colloids Surf. A Physicochem. Eng. Asp. 383, 2–9.
Parsons, D.F., Ninham, B.W., 2012. Nonelectrostatic ionic forces between dissimilar surfaces: a mechanism for colloid separation. J. Phys. Chem. C 116, 7782–7792.
Parsons, D.F., Salis, A., 2015. The impact of the competitive adsorption of ions at surface sites on surface free energies and surface forces. J. Chem. Phys. 142.

Parsons, D.F., Salis, A., 2019. A thermodynamic correction to the theory of competitive chemisorption of ions at surface sites with nonelectrostatic physisorption. J. Chem. Phys. 151.
Peacock, J., Matijević, E., 1980. Precipitation of alkylbenzene sulfonates with metal ions. J. Colloid Interface Sci. 77, 548–554.
Pegram, L.M., Records, M.T., 2007. Hofmeister salt effects on surface tension arise from partitioning of anions and cations between bulk water and the air-water interface. J. Phys. Chem. B 111, 5411–5417.
Prestidge, C.A., Ralston, J., 1995. Contact angle studies of galena particles. J. Colloid Interface Sci. 172, 302–310.
Prestidge, C.A., Ralston, J., 1996. Contact angle studies of ethyl xanthate coated galena particles. J. Colloid Interface Sci. 184, 512–518.
Pugh, R.J., 1988. In: Forsberg, E. (Ed.), Surface Chemical Studies on Sulphide Flotation. Proceedings of XVI International Mineral Processing Congress, Stockholm, June 5-10. Elsevier, Amsterdam, p. 751.
Puigdomenech, I., 2004. Hydra/Medusa Chemical Equilibrium Database and Plotting Software. KTH Royal Institute of Technology.
Quinn, J.J., Kracht, W., Gomez, C.O., Gagnon, C., Finch, J.A., 2014. Comparing the effect of salts and frother (MIBC) on gas dispersion and froth properties. Miner. Eng. 20, 1296–1302.
Ralston, J., 1994. The chemistry of galena flotation: principles and practice. Miner. Eng. 7 (5–6), 715–735.
Ramos, O., Castro, S., Laskowski, J.S., 2013. Copper-molybdenum ores flotation in seawater: floatability and frothability. Miner. Eng. 53, 108–112.
Smith, L.K., Heyes, G.W., 2012. The effect of water quality on the collector-less flotation of chalcopyrite and bornite. In: Third International Congress on Water Management in Mining Industry (Santiago, Chile).
Tadesse, D., Parsons, D.F., 2023. Thermodynamics beyond Dilute Solution Theory: Steric Effects and Electrowetting.
Wang, B., Peng, Y., 2014. The effect of saline water on mineral flotation – a critical review. Miner. Eng. 66–68, 13–24.
Wang, D., Jiao, F., Qin, W., Wang, X., 2017. Effect of surface oxidation on the flotation separation of chalcopyrite and galena using sodium humate as depressant. Separ. Sci. Technol. 53, 961–972.
Wang, J., Li, G., Li, S., Wang, Y., Xing, Y., Ma, Z., Cao, Y., 2019. Investigation on properties of aqueous foams stabilized by aliphatic alcohols and polypropylene glycol. J. Dispersion Sci. Technol. 40, 728–736.
Woods, R., 2003. Electrochemical potential controlling flotation. Int. J. Miner. Process. 72, 151–162.
Woods, R., 1987. In: Somasundaran, P., Moudgil, B.M. (Eds.), Flotation of Sulfide Minerals: Reagents in Mineral Technology. Marcel Dekker, New York, pp. 39–78.
Wu, Z., Wang, X., Liu, H., Zhang, H., D Miller, J., 2016. Some physicochemical aspects of water-soluble mineral flotation. Adv. Colloid Interface Sci. 235, 190–200.
Xing, Y., Gui, X., Karakas, F., Cao, Y., 2017. Role of collectors and depressants in mineral flotation: a theoretical analysis based on extended DLVO theory. Minerals 7, 223–239.
Yang, C., Dabros, T., Li, D., Czarnecki, J., Masliyah, J.H., 2001. Measurement of the zeta potential of gas bubbles in aqueous solutions by microelectrophoresis. J. Colloid Interface Sci. 243, 128–135.
Yoon, R.H., Sabey, J.B., 1989. Coal flotation in inorganic salt solutions. In: Botsaris, G., Glazman, Y.M. (Eds.), International Phenomena in Coal Technology. Dekker, New York.
Young, T., 1805. An essay on the cohesion of fluids. Phil. Trans. Roy. Soc. Lond. 95, 65–87.
Yu, D., Wang, Y., Zhang, J., Tian, M., Han, Y., Wang, Y., 2012. Effects of calcium ions on solubility and aggregation behaviour of an anionic sulfonate gemini surfactant in aqueous solutions. J. Colloid Interface Sci. 381, 83–88.
Zha, L., Li, H., Wang, N., 2020. Electrochemical study of galena weathering in NaCl solution: kinetics and environmental implications. Minerals 10, 416.
Zhang, X.H., Quinn, A., Ducker, W.A., 2008. Nanobubbles at the interface between water and hydrophobic solid. Langmuir 24, 4756–4764.